Inorg. Chem. **2007**, *46*, 6204–6210

Growth of Dumbbell-like ZnO Microcrystals under Mild Conditions and their Photoluminescence Properties

Qingjiang Yu, Cuiling Yu, Haibin Yang,* Wuyou Fu, Lianxia Chang, Jing Xu, Ronghui Wei, Hongdong Li, Hongyang Zhu, Minghui Li, and Guangtian Zou

National Laboratory of Superhard Materials, Jilin University, Changchun, 130012, P. R. China

Guorui Wang, Changlu Shao, and Yichun Liu

Center for Advanced Optoelectronic Functional Material Research, Northeast Normal University, Changchun, 130024, P. R. China

Received January 3, 2007

Large-scale uniform dumbbell-like ZnO microcrystals were successfully synthesized via a facile solution method under mild conditions. The as-prepared dumbbells, with lengths of 3.5–5.4 μm and diameters of 1.3–1.8 μm, possess a single-crystal hexagonal structure and grow along the [0001] direction. The influence of the reactant concentration on the size and shapes of the ZnO samples had been studied, and the results revealed that the reactant concentration plays a crucial role in determining final morphologies of the samples. Moreover, the evolution process of the dumbbell-like ZnO microcrystals was viewed by field-emission scanning electron microscopy (FE-SEM) characterization, and a possible formation mechanism was proposed. In addition, optical properties of the ZnO samples prepared at different reaction times were also investigated by photoluminescence (PL) spectroscopy. The room-temperature PL spectrum of the dumbbell-like ZnO microcrystals shows a strong UV emission peak. The UV emission is further identified to originate from the radiative free-exciton recombination by the temperature-dependent PL.

Introduction

Semiconductor nanomaterials have recently attracted much attention because of their novel properties and potential applications in manufacturing electronic and optoelectric devices.[1−3] Among these materials, ZnO, with a wide direct band gap (3.37 eV) and a large exciton-binding energy (60 meV), is an important semiconducting material that exhibits many interesting properties including near-UV emission,[4] conductivity,[5] piezoelectricity,[6] photocatalysis,[7] and sensitivity to gas.[8] On the basis of the remarkable physical properties and the versatile applications of the ZnO material, a large effort has been focused on the synthesis, characteristics, device fabrication, and performance improvement of the ZnO nano- or microstructures for semiconductor device miniaturization.[3,9]

The control over the size and morphology of nanometer- or micrometer-sized ZnO crystals represents a great challenge to realize the design of novel functional devices. This is because the optical and electronic properties of ZnO crystals, which finally determine practical applications, can be modulated by varying their size and morphology. Recently, the synthesis of one-dimensional ZnO nano- or microstructures in shapes including wires,[3] rods,[10,11] tubes,[12,13] needles,[14]

* To whom correspondence should be addressed. Phone: +86-431-85168763. Fax: +86-431-85168816. E-mail: yanghb@jlu.edu.cn.

(1) Duan, X.; Huang, Y.; Cui, Y.; Wang, J.; Liber, C. M. *Nature* **2001**, *409*, 66.
(2) Cui, Y.; Lieber, C. M. *Science* **2001**, *291*, 851.
(3) Huang, H. M.; Mao, S.; Feick, H.; Yan, H.; Wu, H.; Kind, H.; Weber, E.; Russo, R.; Yang, P. *Science* **2001**, *292*, 1897.
(4) Service, R. F. *Science* **1997**, *276*, 895.
(5) Katoh, R.; Furube, A.; Hara, K.; Murata, S.; Sugihara, H.; Arakawa, H.; Tachiya, M. *J. Phys. Chem. B* **2002**, *106*, 12957.
(6) Minne, S. C.; Manalis, S. R.; Quate, C. F. *Appl. Phys. Lett.* **1995**, *67*, 3918.
(7) Yang, J. L.; An, S. J.; Park, W. I.; Yi, G. C.; Choi, W. Y. *Adv. Mater.* **2004**, *16*, 1661.
(8) Wan, Q.; Li, Q. H.; Chen, Y. J.; Wang, T. H.; He, X. L.; Gao, X. G.; Li, J. P. *Appl. Phys. Lett.* **2004**, *84*, 16.
(9) Fan, Z.; Lu, J. G. *J. Nanosci. Nanotechnol.* **2005**, *5*, 1561.
(10) Guo, L.; Ji, Y. L.; Xu, H. *J. Am. Chem. Soc.* **2002**, *124*, 14864.
(11) Vayssieres, L. *Adv. Mater.* **2003**, *15*, 464.
(12) Vayssieres, L.; Keis, K.; Hagfeldt, A.; Lindquist, S. E. *Chem. Mater.* **2001**, *13*, 4395.

10.1021/ic070008a CCC: $37.00
Published on Web 06/30/2007

columns,[15] towers,[16,17] belts,[18] nails,[19] helices,[20] branches,[21] combs,[22] tetrapods,[23] and dumbbells[24−27] has been of increasing interest because of their promising applications in optoelectronic devices and functional materials. Different methods such as vapor−liquid−solid growth, thermal evaporation, thermal decomposition, electrochemical deposition, and solution-phase processes have been introduced to prepare one-dimensional ZnO nano- or microstructured materials with various morphologies. Large-scale use will require the development of simple low-cost approaches to the synthesis of inorganic functional nanomaterials. Of these methods, the facile solution procedure, may be the most simple and effective way to prepare large-scale and well-crystallized materials at a relatively low temperature.

Recently, dumbbell-like ZnO microcrystals were prepared by a hydrothermal process,[24−25] but the morphologies of the ZnO crystals were controlled by additives. Moreover, the hydrothermal reaction is not suitable for scale-up production because of pressure limitations. Subsequently, Wang and coworkers also fabricated dumbbell-like ZnO microcrystals by an ambient-pressure and low-temperature zerogel-seeded opening crystallization approach,[26] and dumbbell-like ZnO microcrystals were prepared on the ZnO nanorod-built cotton fabrics. However, they did not discuss the basic growth process and presented only the morphology of obtained ZnO microcrystals. Furthermore, the synthesis process was comparatively complicated. Herein, we present a simple wet chemical approach to the fabrication of dumbbell-like ZnO microcrystals without any additives, templates, or substrates at an ambient pressure and low temperature (90 °C). The crystallinity, morphology, and structure of the dumbbell-like ZnO microcrystals are examined; effects of the reactant concentration and the reaction time on the size and shapes of the ZnO products are analyzed, and the formation mechanism of dumbbell-like ZnO microcrystals is discussed from the angle of nucleation and morphology. Furthermore, the room- and low-temperature photoluminescence (PL) of the dumbbell-like ZnO microcrystals were also investigated.

(13) Yu, H.; Zhang, Z.; Han, M.; Hao, X.; Zhu, F. *J. Am. Chem. Soc.* **2005**, *127*, 2378.
(14) Park, W. I.; Yi, G. C.; Kim, M.; Pennycook, S. J. *Adv. Mater.* **2002**, *14*, 1841.
(15) Tian, Z. R.; Voigt, J. A.; Liu, J.; Mckenzie, B.; Mcdermott, M. J. *J. Am. Chem. Soc.* **2002**, *124*, 12954.
(16) Zhang, H.; Yang, D.; Ji, Y.; Ma, X.; Xu, J.; Que, D. *J. Phys. Chem. B.* **2004**, *108*, 3955.
(17) Wang, Z.; Qian, X.; Yin, J.; Zhu, Z. *Langmuir* **2004**, *20*, 3441.
(18) Pan, Z. W.; Dai, Z. R.; Wang, Z. L. *Science* **2001**, *291*, 1947.
(19) Lao, J. Y.; Huang, J. Y.; Wang, D. Z.; Ren, Z. F. *Nano Lett.* **2003**, *3*, 235.
(20) Kong, X. Y.; Wang, Z. L. *Nano Lett.* **2003**, *3*, 1625.
(21) Milliron, D. J.; Hughes, S. T.; Cui, Y.; Manna, L.; Li, J.; Wang, L. W.; Alivisatos, A. P. *Nature* **2004**, *430*, 190.
(22) Yan, H.; He, R.; Johnson, J.; Law, M.; Saykally, R. J.; Yang, P. *J. Am. Chem. Soc.* **2003**, *125*, 4728.
(23) Dai, Y.; Zhang, Y.; Li, Q. K.; Nan, C. W. *Chem. Phys. Lett.* **2002**, *358*, 83.
(24) Wang, B. G.; Shi, E. W.; Zhong, W. Z. *Cryst. Res. Technol.* **1998**, *33*, 937.
(25) Zhang, H.; Yang, D.; Li, D.; Ma, X.; Li, S.; Que, D. *Cryst. Growth Des.* **2004**, *5*, 547.
(26) Wang, R. H.; Xin, J. H.; Tao, X. M.; Daoud, W. A. *Chem. Phys. Lett.* **2004**, *398*, 250.
(27) Govender, K.; Boyle, D. S.; Kenway, P. B.; O' Brien, P. *J. Mater. Chem.* **2004**, *14*, 2575.

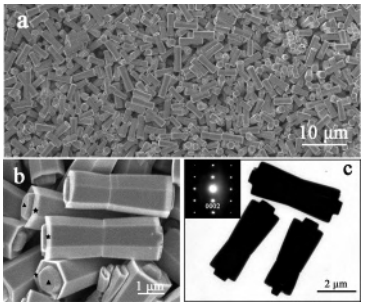

Figure 1. FE-SEM and TEM images of the dumbbell-like ZnO sample: (a) low-resolution image, (b) high-resolution image, and (c) TEM image and SAED pattern (inset) of the sample.

Experimental Section

All chemicals (analytical grade reagents) were purchased from Beijing Chemicals Co. Ltd. and were used as received without further purification. Deionized water with a resistivity of 18.0 MΩ cm was used in all experiments. In a typical synthesis process, 100 mL of aqueous solution of zinc acetate dihydrate ($Zn(CH_3COO)_2 \cdot 2H_2O$) and 100 mL of hexamethylenetetramine ($(CH_2)_6N_4$, HMT) aqueous solution of equal concentration (0.1 M) were mixed together and kept under mild magnetic stirring for 5 min. Then the solution was transferred into a 500 mL flask and heated at 90 °C for 2 h with refluxing. Subsequently, the resulting white products were centrifuged, washed with deionized water and ethanol, and dried at 60 °C in air for further characterization.

X-ray power diffraction (XRD) analysis was conducted on a Rigaku D/max-2500 X-ray diffractometer with Cu Kα radiation (λ = 1.5418 Å). Field-emission scanning electron microscopic images were performed on a JEOL JEM-6700F microscope operating at 5 KV. Transmission electron microscope (TEM) images and the selected area electron diffraction (SAED) patterns were obtained on a JEOL JEM-2000EX microscope with an accelerating voltage of 200 kV. Raman-scattering spectra were measured by HR-800 LabRam confocal Raman microscope with a backscattering configuration made by JY company in France, excited by the 514 nm line of an argon-ion laser at room temperature. The PL emission spectra were recorded with HR-800 LabRam Infinity Spectrophotometer excited by a continuous He−Cd laser with a wavelength of 325 nm.

Results and Discussion

Structure and Morphology. The morphology of the obtained ZnO was characterized by FE-SEM and TEM, and typical images are shown in Figure 1. The low-resolution image (Figure 1a) shows that the sample is a typical dumbbell structure composed of two hexagonal prisms. The as-prepared dumbbells were 3.5−5.4 μm in length and 1.3−1.8 μm in diameter. The high-resolution image in Figure 1b clearly reveals that the obtained ZnO exhibits the well-defined dumbbell-like morphology. It can be obviously seen that smaller columns, with lengths of 200−400 nm and diameters of 200−800 nm, and hexagonal rings, with lengths of 100−200 nm and wall thickness of 20−30 nm, grew on the center and edge of end faces of the prepared dumbbells, as indicated by the triangles and the stars, respectively. This is obvious differences in the dumbbell-like ZnO structures reported.[24−27] Further morphology characterization of the ZnO sample was performed on a transmission electron microscope as shown in Figure 1c, which agrees with the

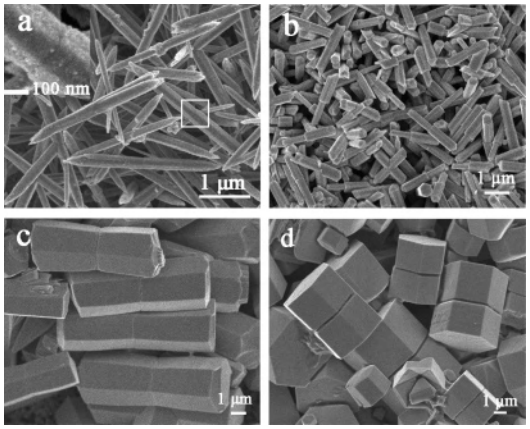

Figure 2. FE-SEM images of the synthesized ZnO samples with different reactant concentrations: (a) 0.025, (b) 0.05, (c) 0.2, and (d) 0.5 M. The reaction time is 2 h.

FE-SEM results. The inset SAED pattern indicates that the dumbbells possess a single-crystal hexagonal structure and grow along the [0001] direction.

To investigate the effects of the reactant concentration, we simply changed the concentration of the $Zn(CH_3COO)_2$ and HMT while keeping their ratio constant. Figure 2 displays the morphologies of the synthesized ZnO samples at different reactant concentrations. When the reactant concentration was 0.025 M, the obtained ZnO sample exhibited the typical bipyramidal microrod structure with an aspect ratio of 13−18 and a diameter of 100−300 nm. Furthermore, the grain boundary was observed at the middle part of the bipyramidal microrod, as shown in the inset which is the high-resolution image of the area of the rectangle in Figure 2a, which implys that the bipyramidal microrod consists of two ZnO microrods, namely, a twinned rod. When the concentration was increased to 0.05 M, the obtained ZnO sample displayed the twinned prism structure, but the twinned prisms were asymmetrical. Once the concentration was increased to 0.1 M, monodisperse, dumbbell-like ZnO microcrystals were successfully obtained, as illustrated in Figure 1. As the concentration was increased to 0.2 M, the dumbbell-like ZnO microcrystals grew larger and longer. When the concentration was further increased to 0.5 M, the typical twinned hexagonal prisms (Figure 2d), with an aspect ratio of 1−1.3 and diameter of 3.6−5.5 μm, were achieved, and the two end planes of the twinned prisms were very flat. It is found that the volume of the obtained ZnO products obviously increased with increasing the reactant concentration. This is because that the higher the reactant concentration, the more ZnO nuclei appear simultaneously at the beginning of the reaction. These nuclei congregate easily and form bigger nuclei under hydrothermal conditions, leading to the formation of bigger ZnO crystals. Moreover, it is also found that the aspect ratio of the obtained ZnO samples gradually decreased with an increase in the reactant concentration. That is to say, the ZnO preferential growth difference between (0001) and other directions would diminish with an increase in the reactant concentration. The possible reason will be described below in detail.

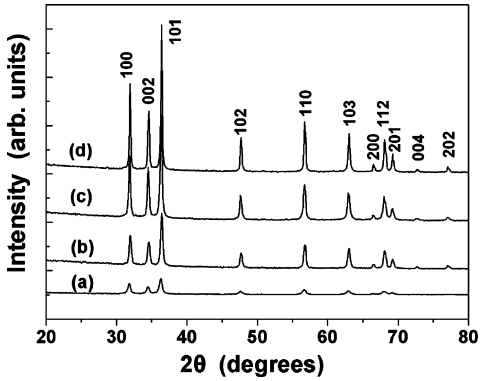

Figure 3. XRD patterns of the ZnO samples obtained at different reaction times: (a) 10 min, (b) 30 min, (c) 1 h, and (d) 2 h. The reactant concentration is 0.1 M.

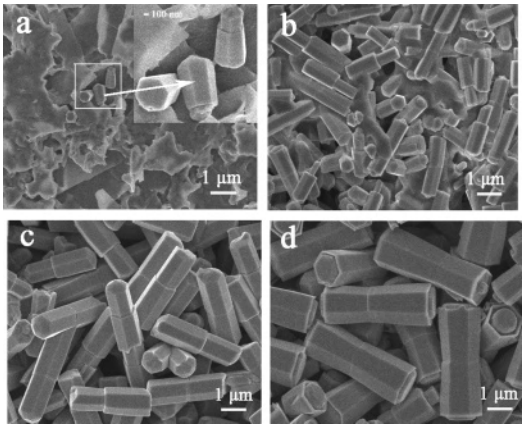

Figure 4. FE-SEM images of the ZnO samples prepared at different reaction times: (a) 10 min, (b) 30 min, (c) 1 h, and (d) 2 h. The reactant concentration is 0.1 M.

Morphology Evolution. To understand the growth mechanism of the dumbbell-like ZnO microcrystals, the ZnO samples were collected after 10 min, 30 min, 1 h, and 2 h for XRD and FE-SEM characterization. Figure 3 shows XRD patterns of the ZnO samples obtained at different reaction times. It can be seen that the diffraction peaks of each sample display a wurtzite structure (hexagonal phase, space group $P6_3mc$) and are in good agreement with the JCPDS file of ZnO (JCPDS 36-1451). No impurities were observed in these patterns. Moreover, the intensities of the diffraction peaks increased with an increase in the reaction time. This means that the longer reaction time leads to higher crystal quality.

Figure 4 shows the evolution of the ZnO structures as a function of reaction time. The FE-SEM observation of the sample which aged at 90 °C for only 10 min revealed that a few hexagonal cones, about 400 nm in diameter and 900 nm in length, were randomly scattered in the floccules, as illustrated in Figure 4a. As seen from the XRD pattern of the sample prepared at the reaction time of 10 min in Figure 3 and the TEM image in the inset of Figure 6, the floccules are actually ZnO nanoparticles with an average diameter of 4 nm. In addition, the inset which is the high-resolution image of the area of the rectangle in Figure 4a clearly shows that smaller one end of the cones grew out a "bud". This is

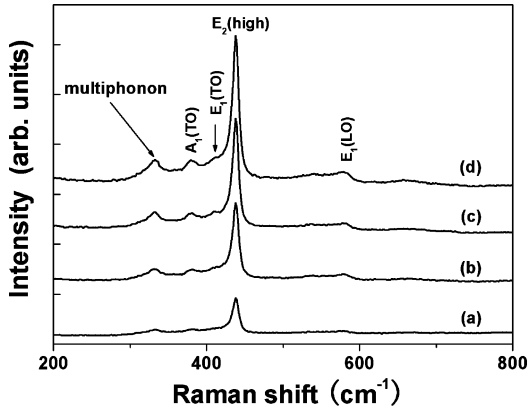

Figure 5. Raman spectra of the ZnO samples prepared at different reaction times: (a) 10 min, (b) 30 min, (c) 1 h, and (d) 2 h. The reactant concentration is 0.1 M.

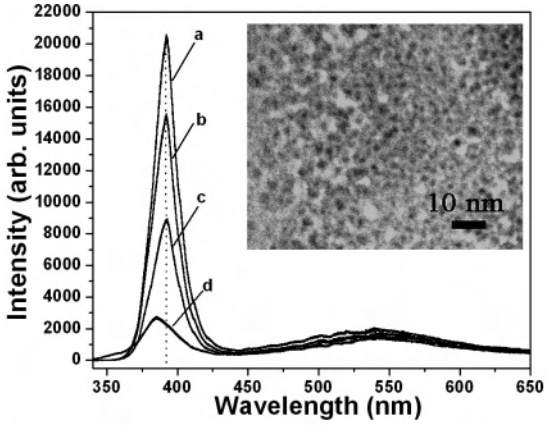

Figure 6. Room-temperature PL spectra of the ZnO samples prepared at different reaction times: (a) 10 min, (b) 30 min, (c) 1 h, and (d) 2 h. The reactant concentration is 0.1 M. The inset is the TEM image of the ZnO nanoparticles with the reaction time of 10 min.

similar to the early growth process of ZnO troughs.[28] As the reaction time was prolonged to 30 min, ZnO nanoparticles decreased, while twinned hexagonal prisms obviously increased (Figure 4b). This suggests that ZnO nanoparticles are only an intermediate and will gradually form twinned prisms as the reaction time increases. The twinned prisms were asymmetrical because one subunit was larger than the other. It is apparent that the larger and smaller subunits of the twinning derived from the cone and the bud, respectively. When the reaction proceeded to 1 h, the twinned prisms grew larger and longer and showed better crystal perfection. Moreover, there were two well-developed ZnO $(000\bar{1})$ planes at the grain boundary, which provide some clues for the understanding of the growth mechanism. When the reaction was further prolonged to 2 h, the smaller subunit of the twinning had evolved to be equivalent with the bigger one, and typical dumbbell-like ZnO microcrystals came into being, as shown in Figure 4d. The effect of longer reaction times, up to 6 h, was also investigated. Results show that reaction time exceeding 2 h will not bring about evident structural and morphological modifications. Therefore, a reaction time of 2 h is sufficient to obtain the well-defined dumbbell-like ZnO microcrystals.

Raman spectroscopy was also carried out to study the vibrational properties of the ZnO samples prepared at different reaction times. Figure 5 presents the Raman spectra of these samples at the range of 200−800 cm^{-1}. The dominant feature at 438 cm^{-1} is the result of ZnO nonpolar optical phonons E_2(high) mode. The E_2(high) mode corresponds to characteristic band of hexagonal wurtzite phase. It is found that the E_2(high) mode becomes stronger when the reaction time increases, which may mean improved crystallinity of the prepared ZnO samples. The peaks at 382 and 413 cm^{-1} correspond to A_1(TO) and E_1(TO) phonons of ZnO crystal, respectively. In addition, the E_1(LO) peak can also be observed at 576 cm^{-1}. The appearance of the E_1(LO) peak has been attributed to the formation of defects such as oxygen vacancy, zinc interstitial, or their complexes.[29] According to Figure 5, the E_2(high) peak shows a dominant intensity over the E_1(LO) peak and a very sharp feature. It indicates that ZnO crystal quality is very good, which is in agreement with XRD result. The peak located at 332 cm^{-1} may be attributed to a multiphonon scattering process ($E_{2H} - E_{2L}$).[30]

Growth Mechanism. The overall reaction for the growth of ZnO crystals may be simply formulated as follows:

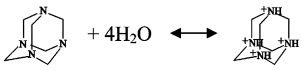

(1)

$$Zn^{2+} + 4OH^- \leftrightarrow ZnO_2^{2-} + 2H_2O \quad (2)$$

$$ZnO_2^{2-} + 2H_2O \leftrightarrow ZnO + 2OH^- \quad (3)$$

In the synthesis systems, HMT serves as a pH buffer to release OH^-; OH^- subsequently reacts with Zn^{2+} to form ZnO_2^{2-}, and finally the formation of ZnO is largely via homogeneous precipitation under mild conditions.

To understand the observed behaviors of ZnO, it is necessary to investigate its growth mechanism. It is well-known that the hexagonal ZnO crystal has both polar and nonpolar faces. The typical crystal habit exhibits a basal polar oxygen plane $(000\bar{1})$, a top tetrahedron corner-exposed polar zinc plane (0001), and low-index faces (parallel to the *c*-axis) consisting of a nonpolar $\{10\ \bar{1}\ 0\}$ face. Polar faces with surface dipoles are thermodynamically less stable than nonpolar faces, often undergo rearrangement to reduce their surface energy.[27] At the early stage of the reaction system, ZnO_2^{2-} ions, the growth units in the solution near the surface of the ZnO nanoparticles are likely adsorbed on the positive polar face of the (0001) surface, resulting in faster growth along the [0001] direction, and thus solid ZnO cones were obtained. Moreover, HMT will hydrolyze in the aqueous solution and form the $(CH_2)_6N_4-4H^+$ complex (abbreviated as HMT−H4) according to eq 1,[31] which bears four positive

(28) Tang, J.; Cui, X.; Liu, Y.; Yang, X. *J. Phys. Chem. B* **2005**, *109*, 22244.

(29) Pradhan, A. K.; Zhang, K.; Loutts, G. B.; Roy, U. N.; Cui, Y.; Burger, A. *J. Phys.: Condens. Matter* **2004**, *16*, 7123.
(30) Damen, T. C.; Porto, S. P. S.; Tell, B. *Phys. Rev.* **1966**, *142*, 570.
(31) Gao, X.; Li, X.; Yu, W. *J. Phys. Chem. B* **2005**, *109*, 1155.

charges. Thus, by the coulomb interaction, the HMT−H4 complex would adsorb on the negative polar face of the $(000\bar{1})$ surface. While the HMT−H4 complex would also adsorb ZnO_2^{2-} ions, and thus the smaller end of the cones grew out a bud. The cones and buds gradually grew larger and longer with an increase in the reaction time and finally formed typical dumbbell-like ZnO microcrystals. In addition, it is a very interesting phenomenon that some small columns grow on the center of the end faces of the dumbbell-like ZnO microcrystals. Wei et al.[32] have reported that ZnO nanorod arrays were first dissolved on the center of the metastable (0001) planes of the rods during the aging process, leading to the formation of tubular ZnO structures. This indicates that the atoms are the most unstable on the center of the metastable (0001) planes of the rods. Therefore, the precursor ZnO_2^{2-} is very easily deposited on the center of the metastable (0001) planes of the dumbbells. Since the concentration of ZnO_2^{2-} was very low after the formation of the symmetrical dumbbells, the smaller columns finally formed on the center of the two ends of the dumbbells. The formation mechanism of the hexagonal rings on the edge of the dumbbells is not yet clear and warrants further investigation, and a related study is underway. Moreover, in the solution, CH_3COO^- ions may also be adsorbed on the positive polar face of the (0001) surface. When the reactant concentration (0.025 M) is lower, the concentration of CH_3COO^- ions is also lower, and the adsorption of ZnO_2^{2-} ions on the (0001) surface are dominant, thus resulting in the faster growth rate along the [0001] direction than those along other directions, therefore, the ends of the rods become cuspate as shown in Figure 2a. In contrast, when the reactant concentration (0.5 M) is higher, many of ZnO nuclei appear simultaneously at the beginning of the reaction. With the reaction going on, the concentration of ZnO_2^{2-} ions rapidly reduces. While the concentration of CH_3COO^- ions is still higher, CH_3COO^- ions will compete with ZnO_2^{2-} ions to absorb on the (0001) surface, which prevents the contact of ZnO_2^{2-} on the (0001) surface and thus limits the crystal growth along the [0001] direction;[33] therefore, the ends of the rods become flat as shown in Figure 2d. The top of the small columns at the ends of the dumbbells is flat, which may also be due to the effect of CH_3COO^- ions.

Photoluminescence. The PL from ZnO consists of two emission bands at room temperature: a near-band-edge (UV) emission and a broad, deep-level (visible) emission. The visible emission is usually considered to be related to various intrinsic defects produced during ZnO preparation.[34,35] Normally, these defects are located at the surface of the ZnO structure.[34−36] Figure 6 shows the PL spectra of the ZnO samples prepared at different reaction times, which is excited by 325 nm UV light from He−Cd laser at room temperature. The PL spectra of the samples prepared at reaction times of 30 min, 1 h, and 2 h revealed similar features. There appeared a strong UV emission at ~392 nm and a weak broad green emission around 540 nm. The UV emission is the band-edge emission resulting from the recombination of free excitons. Though the origin of the green emission is controversial, generally it is attributed to the singly ionized oxygen vacancy, and the emission results from the radiative recombination of a photogenerated hole with electron occupying the oxygen vacancy.[37] Compared with the ZnO samples prepared at reaction times of 30 min, 1 h, and 2 h, the UV emission peak position of the ZnO sample with the reaction time of 10 min has a blue shift to higher energy and is located at ~384 nm. The ZnO sample with the reaction time of 10 min is mostly nanoparticles with an average diameter of 4 nm, as shown in the inset of Figure 6. The blueshift behavior of the UV emission peak position may be explained by the effect of quantum confinement. In general, quantum confinement will widen the energy and give rise to a blueshift in the transition energy as the crystal size decreases.[38] Although there are a few nanoparticals with an average diameter of 4 nm in the ZnO sample with the reaction time of 30 min, the twinned prisms are dominant. This may result in the UV emission peak position of the ZnO sample with the reaction time of 30 min having no blueshift. The intensity ratio of the UV emission and the visible emission of the ZnO samples with the reaction time of 10 min, 30 min, 1 h, and 2 h are 1.74, 5.49, 8.83, and 10.43, respectively. This indicates that the crystal quality of the ZnO samples gets better with increasing the reaction time, which is consistent with the result of XRD in Figure 3. Sun et al.[39] in their excellent work reported that the intensity ratio of the UV emission and the visible emission of ZnO nanorods and nanotubes were 0.32 and 3.4, respectively. Compared with their results, the dumbbell-like ZnO microcrystals prepared at the reaction time of 2 h have the best crystal quality. In addition, when the dumbbell-like ZnO microcrystals with the reaction time of 2 h were annealed at 300 °C in air for 1 h, the morphology of the microcrystals did not change, as shown in the inset of Figure 7. Compared with the unannealed ZnO microcrystals, the UV emission intensity of the annealed ZnO microcrystals drastically increased without changing its position, the intensity of the green emission obviously decreased, as shown in Figure 7. This result can be attributed to the decrease in the amount of the singly ionized oxygen vacancies in the ZnO. The intensity ratio of the UV emission and the visible emission of the annealed dumbbell-like ZnO microcrystals is 43.56, which suggests that good crystal quality of dumbbell-like ZnO microcrystals can be produced via a simple and comparatively low-temperature heat-treatment process.

To better understand PL property of the dumbbell-like ZnO microcrystals, the PL spectrum measured at 80 K is shown

(32) Wei, A.; Sun, X. W.; Xu, C. X.; Dong, Z. L.; Yang, Y.; Tan, S. T.; Huang, W. *Nanotechnology* **2006**, *17*, 1740.
(33) Xu, L.; Guo, Y.; Liao, Q.; Zhang, J.; Xu, D. *J. Phys. Chem. B* **2005**, *109*, 13519.
(34) Hsu, N. E.; Hung, W. K.; Chen, Y. F. *J. Appl Phys.* **2004**, *96*, 4671.
(35) Li, D.; Leung, Y. H.; Djurisic, A. B.; Liu, Z. T.; Xie, M. H.; Shi, S. L.; Xu, S. J.; Chan, W. K. *Appl. Phys. Lett.* **2004**, *85*, 1601.
(36) Shalish, I.; Temkin, H.; Narayanamurti, V. *Phys. Rev. B* **2004**, *69*, 245401.
(37) Vanheusden, K.; Warren, W. L.; Seager, C. H.; Tallant, D. R.; Voigt, J. A.; Gnade, B. E. *J. Appl. Phys.* **1996**, *79*, 7983.
(38) Lin, K. F.; Cheng, H. M.; Hsu, H. C.; Hsieh, W. F. *Appl. Phys. Lett.* **2006**, *88*, 263117.
(39) Sun, Y.; Fuge, M. G.; Fox, N. A.; Riley, D. R.; Ashfold, M. N. R. *Adv. Mater.* **2005**, *17*, 2477.

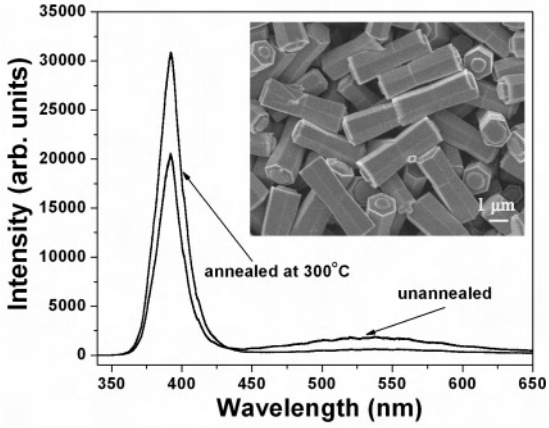

Figure 7. Room-temperature PL spectra of the dumbbell-like ZnO microcrystals with the reaction time of 2 h before and after thermal annealing at 300 °C in air for 1 h. The inset is the FE-SEM image of the annealed ZnO microcrystals.

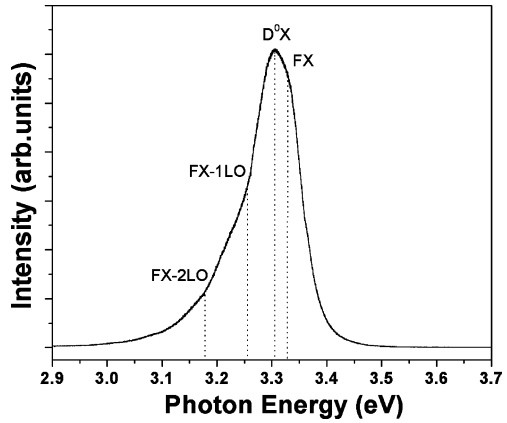

Figure 8. PL spectrum of the dumbbell-like ZnO microcrystals at 80 K.

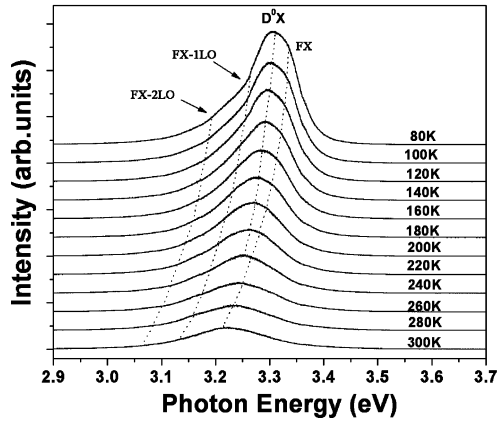

Figure 9. Temperature-dependent PL spectra of the dumbbell-like ZnO microcrystals.

in the Figure 8. The dominant peak at 3.308 eV is known as the donor bound exciton (D^0X) emission.[40] The emission observed at 3.331 eV on the higher-energy shoulder of the D^0X peak is assigned to the free exciton (FX) emission. The lower-energy side of the D^0X peak arises two shoulders located at 3.258 and 3.187 eV, which are attributed to the 1-LO and 2-LO photon replica of FX, respectively.

(40) Wang, D.; Liu, Y. C.; Mu, R.; Zhang, J. Y.; Lu, Y. M.; Shen, D. Z.; Fan, X. W. *J. Phys.: Condens. Matter.* **2004**, *16*, 4635.

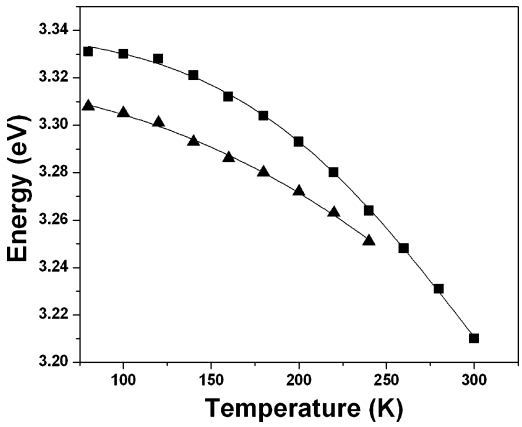

Figure 10. Temperature dependence of excitonic emission energies of the dumbbell-like ZnO microcrystals: ■ and ▲ represent FX and D^0X emissions, respectively.

Figure 9 shows the temperature-dependent PL spectra of the dumbbell-like ZnO microcrystals measured from 80 to 300 K. With the increase of measurement temperature, the intensities of all emissions are decreased and the intensity of the D^0X emission decreases more rapidly than that of the FX emission. The decrease in intensity is the result of the thermal ionization of the bound excitons. The FX emission becomes dominant in the PL spectra when the measurement temperature is above 240 K. In addition, the exciton emission of FX and D^0X show an obvious redshift with increasing measurement temperature. The temperature dependence of the peak energy of FX and D^0X is show in Figure 10. The temperature dependence of the exciton emission energy is related to the temperature dependence of the band energy, which fits well with the semiempirical formula

$$E_x(T) = E_x(0) - \alpha T^2/(T + \beta)$$

where $E_x(0)$ is the peak energy at absolute zero temperature and α and β are the fitting parameters.[41] $E_x(0)$ is 3.334 and 3.312 eV for FX and D^0X emissions, respectively. In Figure 10, the lines represent the calculated temperature dependences for each emission mode, and it is shown that the calculated lines fit well with the experimental values.

Conclusion

In summary, large-scale uniform dumbbell-like ZnO microcrystals have been successfully synthesized via a facile solution method under mild conditions without any additives, templates, or substrates. The as-prepared dumbbells, composed of two hexagonal prisms, possess a single-crystal hexagonal structure and grow along the [0001] direction. The influence of the reactant concentration on the size and shapes of the ZnO products is studied, and the results reveals that the ZnO preferential growth difference between (0001) and other directions will diminish with an increase in the reaction concentration. The growth process and growth mechanism of the dumbbell-like ZnO microcrystals are discussed from

(41) Varshni, Y. P. *Physica* **1967**, *34*, 149.

the angle of nucleation and morphology. The room-temperature PL indicates that the dumbbell-like ZnO microcrystals have a very strong UV emission at ~392 nm, while the low-temperature PL shows that primary emission is from bound and free exciton recombination. The dumbbell-like ZnO microcrystals have promise in their potential application to microscale optoelectronic devices because of their excellent UV emission properties.

IC070008A